THE JOURNAL OF PHYSICAL CHEMISTRY B

Article

pubs.acs.org/JPCB

Aqueous-Biamphiphilic Ionic Liquid Systems: Self-Assembly and Synthesis of Gold Nanocrystals/Microplates

K. Srinivasa Rao, Tushar J. Trivedi, and Arvind Kumar*

CSIR-Central Salt and Marine Chemicals Research Institute, Council of Scientific and Industrial Research (CSIR), G. B. Marg, Bhavnagar 364002, Gujarat, India

Supporting Information

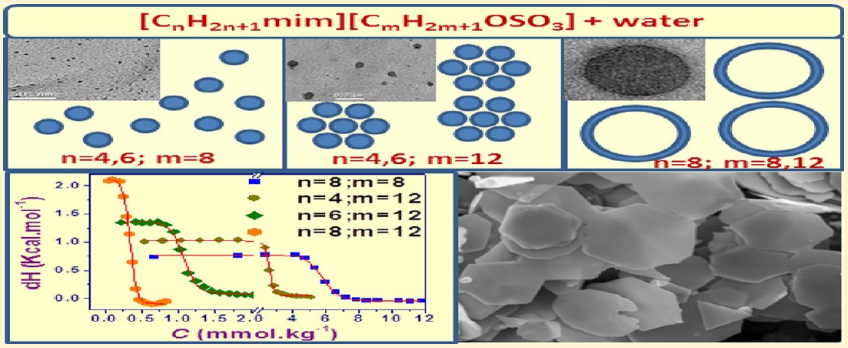

ABSTRACT: Biamphiphilic ionic liquids (BAILs) based on 1,3-dialkylimidazolium cation and alkyl sulfate anions ($[C_nH_{2n+1}mim][C_mH_{2m+1}OSO_3]$; n = 4, 6, or 8; m = 8, 12) have been synthesized and characterized for their self-assembling behavior in the aqueous medium. Effects of alteration of alkyl chain length in cation and anion on surfactant properties of BAILs have been examined from surface tension measurements. The effectiveness of surface tension reduction for BAILs has been found to be exceptionally higher as compared to single chain surface active ILs/conventional surfactants. The thermodynamics of the aggregation process has been studied using isothermal titration calorimetry (ITC) and temperature dependent conductivity experiments. Dynamic light scattering (DLS), nuclear magnetic resonance (NMR), and transmission electron microscopy (TEM) studies showed that BAILs formed distinct aggregated structures depending upon the amphiphilic character present in the cation and anion. BAILs ($[C_nH_{2n+1}mim][C_mH_{2m+1}OSO_3]$) form micelles when n = 4, 6; m = 8, intermicellar aggregates when n = 4, 6; m = 12, and vesicles when n = 8; m = 8, 12. Gold nanoparticles and microplates have been synthesized in micellar and vesicle solutions of BAILs using a simple photoreduction method. The studies show the potential of BAILs for constructing micelles and supramolecular assemblies, such as bilayer vesicles, which are effective in preparation of nanomaterials of controlled size and morphology.

1. INTRODUCTION

Ionic liquids (ILs) are liquids composed entirely of ions and melts below 100 °C; they generally contain large (asymmetric) organic cations with a variety of anions.[1,2] The physicochemical properties of ILs can be modified and tuned for desired applications by simple variations in constituent ions, and hence, these are popularly considered as designer solvents.[3] Surfactant-like ILs can be made by incorporation of amphiphilic character in the constituent ions. In fact, the earlier studies on ILs containing a 1-alkyl-3-methyl imidazolium moiety with a carbon chain length of four and higher or an anion having n-octyl and higher alkyl chain moiety have shown to behave like surfactants and form well-defined aggregated structures in an aqueous medium.[4,5] On the basis of these preliminary studies, several surface active ionic liquids (SAILs) were synthesized and their aggregation behavior was investigated in aqueous and IL media.[6−33] These studies revealed that long chain imidazolium ILs while acting as ionic surfactants show a somewhat superior surface activity, better solubility in a variety of media, and versatility in functionalization as compared to that of traditional ionic surfactants.[21,23,30] A comparatively higher solubility and surface activity of SAILs in various solvents made them better emulsifying agents for the preparation of microemulsions.[34,35] SAILs have also been explored in other applications such as formulation of aqueous biphasic systems for separations,[36,37] as a promotor in organic synthesis,[38] or as promising capping/stabilizing agents in the synthesis of nanomaterials.[39−42]

The substituents on the imidazolium cation, substitution at the alkyl chain, and nature of the counterion have shown a remarkable influence on the aggregation behavior of ILs.[12,19,20,24] It has been shown that the surface activity can be enhanced and supramolecular structures can be formed by mixing of SAILs, such as $[C_6Py][BF_4]$, $[C_6Py][Br]$, or $[C_{12}mim][Br]$, with a conventional surfactant sodium lauryl

Received: October 1, 2012
Revised: November 15, 2012
Published: November 21, 2012

sulfate.[43,44] In a recent study, we have demonstrated that, like mixed cationic and anionic surfactant systems, the mixing of two SAILs ($[C_4mim][C_8OSO_3]$ and $[C_8mim][Cl]$) (mim: methyl imidazolium) in different proportions can lead to formation of micelles and vesicles.[45] The supramolecular structures generated from such systems were effectively used for synthesis of hollow silica spheres and anisotropic gold nanostructures.[34,45]

Observation of dual transitions in various physical properties during the investigations on the aggregation behavior of 1-butyl-3-methylimidazolium octyl sulfate, $[C_4mim][C_8OSO_3]$, in aqueous medium[46] prompted us to design and study the self-assembling behavior of ILs having amphiphilic character in both the constituent ions. Henceforth, we will term such ILs as biamphiphilic ionic liquids (BAILs). The BAILs will behave as catanionic surfactants with improved surface activity and capability of forming a variety of self-assembled structures. Recently, the BAILs based on systematic variation in alkyl chain length of 1,3-dialkylimidazolium cation and alkyl sulfate or sulfonate anions have been reported.[47−49] Obliosca et al.[47] synthesized a series of 1-alkyl-3-methylimidazolium lauryl sulfates and characterized their absorption and photoluminescence properties. Santos et al.[48] investigated the alkyl chain interactions of 1,3-dialkylimidazolium cation and alkyl sulfate ILs at the gas−liquid interface using sum frequency generation studies and concluded that the surface is dominated by an alkyl functional group. Mesomorphism of 1,3-dialkylimidazolium cation and alkyl sulfonate anion ILs using X-ray scattering, polarizing optical microscopy, and differential scanning calorimetry has been investigated by Blesic et al.[49] In the same article, self-aggregation and surface adsorption characteristics of synthesized ILs in an aqueous medium using surface tension and fluorescence spectroscopy with pyrene as a probe molecule is reported. These studies demonstrated that a synergetic packing effect is responsible for lowering CMC values and enhanced surface activity. However, none of these studies shed light on the formation and stability of distinct self-assembled structures formed by the BAILs when the amphiphilicity of either the cation or anion is tailored.

In the present work, we synthesized a series of BAILs, based on 1-alkyl-3-methylimidazolium cation and alkyl sulfates as anion, and studied their self-assembling behavior in aqueous medium. The role of the alkyl chain length of the cation or anion on the formation of micelles, aggregated micelles, and vesicles has been defined, and a detailed study has been carried out to understand the superior surface active characteristics and aggregation thermodynamics of the synthesized BAILs. Self-assembeled BAIL media has been used to produce gold nanoparticles/microplates through a photoreduction method. The morphology and crystallinity of synthesized nanomaterials has been examined through SEM and XRD techniques.

2. EXPERIMENTAL SECTION

2.1. Materials. 1-Bromo butane, 1-bromo hexane, and 1-bromo octane of >98% purity were purchased from SRL, India. 1-Methyl imidazole and sodium octyl sulfate (SOS) of AR grade were purchased from Spectrochem, India. Sodium dodecyl sulfate (SDS) was purchased from Sigma-Aldrich, Germany. Ethyl acetate and dichloromethane of AR grade were procured from SD-fine chem. Ltd., India.

2.2. Synthesis of BAILs. *i. Synthesis of 1-Alkyl-3methyl Imidazolium Bromide.* An equimolar mixture of 1-methyl imidazole and 1-bromo alkane was dissolved in water in a two-necked RBF and kept under reflux conditions for 3 h. Reaction was monitored with TLC. After completion of reaction, water was removed using a rotary evaporator and the product was washed with ethyl acetate three times. Alkyl imidazolium bromide thus obtained was dried and characterized using ^1H NMR and LC-MS techniques.

ii. Synthesis of 1-Alkyl-3-methyl Imidazolium Octyl Sulfate or Lauryl Sulfate Ionic Liquids. An equimolar mixture of alkyl imidazolium bromide and sodium alkyl sulfate salt was dissolved in water and kept at 60 °C for 4 h. Reaction was monitored with TLC. Water was removed from the reaction mixture after completion of reaction using a rotary evaporator. The product was extracted with dichloromethane (DCM), and solid salt (NaBr) was filtered off. The product was washed with water several times until complete removal of chloride ions (monitored with acidic solution of $AgNO_3$) and completely dried prior to use. The NMR analysis of the synthesized BAILs is given in the Supporting Information.

2.3. Methods. *2.3.1. Tensiometry.* Surface tension measurements were carried out at 298.15 K using a Data Physics DCAT-II automated Tensiometer employing the Wilhelmy plate method. Aliquots of BAIL stock solutions were added to Millipore grade water by weight and stirred for about 10 min for complete solubilization. Prior to measurements, the resultant solutions were kept for at least 10 min for equilibration. The data was collected in triplicate and was found to be accurate within 0.1 mN m^{-1}. The temperature of the measurement cell was controlled with a Julabo water thermostat to within 0.1 K.

2.3.2. Conductometry. Specific conductivity was measured at four different temperatures in a temperature range of 288.15−318.15 K at 10 K intervals by a digital conductivity meter (Systronics 308) using a cell with a unit cell constant. The temperature of the measurement cell was controlled with a Julabo water thermostat to within 0.1 K. The conductivity after each addition was measured by adding aliquots of concentrated BAILs aqueous solutions to a conductivity cell containing water. Measurements were performed with an uncertainty of less than 0.5%.

2.3.3. Isothermal Titration Calorimetry (ITC). Calorimetric titration was performed with a MicroCal ITC200 microcalorimeter. The sample and reference cells were filled with Millipore water and stabilized at 298.15 K. 40 μL of BAIL stock solutions prepared in water were taken in an instrument controlled Hamiltonian syringe, and 2 μL aliquots were added to the sample cell containing 200 μL of water with continuous stirring (500 rpm). The parameters like time of addition and duration between each addition were controlled by software provided with the instrument. The enthalpy change at each injection was measured and plotted against concentration by using origin software provided with the instrument.

2.3.4. Dynamic Light Scattering (DLS). DLS measurements were performed at 298.15 K by using a NaBiTec Spectro-Size300 light scattering apparatus (NaBiTec, Germany) with a He−Ne laser (633 nm, 4 M_w). BAIL solutions of a concentration above the CAC (~10 times the CAC) were filtered directly into the quartz cell using a membrane filter of 0.45 μm pore size. Prior to measurements, the quartz cell was rinsed several times with filtered water and then filled with filtered sample solutions. The temperature of the measurements was controlled with an accuracy of 0.1 K. The data evaluation of the dynamic light scattering measurements was performed with the inbuilt CONTIN algorithm.

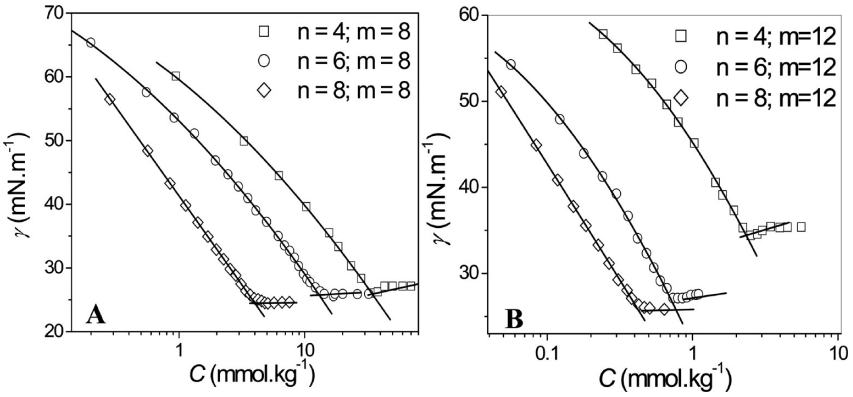

Figure 1. Plots of surface tension as a function of concentration of BAILs ($[C_nH_{2n+1}mim][C_mH_{2m+1}OSO_3]$) in aqueous solutions at 298.15 K.

Table 1. Critical Aggregation Concentration (CAC), Surface Tension at CAC (γ_{CAC}), Adsorption Efficiency (pC_{20}), Effective Surface Tension Reduction (Π_{CAC}), Maximum Surface Excess Concentration (Γ_{max}), and Area Occupied by a Single Molecule at the Air−Water Interface (A_{min}) of BAILs in Aqueous Medium at 298.15 K

$[C_nH_{2n+1}mim][C_mH_{2m+1}OSO_3]$							
n	m	CAC ($mmol·kg^{-1}$)	γ_{CAC} ($mN·m^{-1}$)	pC_{20}	Π_{cac} ($mN·m^{-1}$)	Γ_{max} ($\mu mol·m^{-2}$)	A_{min} (Å^2)
4	8	34.9	26.1	2.5	45.9	1.9	87.1
6	8	14.2	25.6	2.9	45.2	1.9	84.7
8	8	4.1	24.4	3.3	47.6	2.5	66.0
4	12	2.4	34.4	3.3	37.6	2.4	67.8
6	12	1.1	27.1	4.1	44.9	2.4	68.5
8	12	0.4	26.0	4.3	46.0	2.4	68.5

2.3.5. Nuclear Magnetic Resonance (NMR). The ^1H NMR spectra of aqueous BAIL solutions were recorded in a Bruker 500 MHz spectrometer using C_6D_6 as an external solvent.

2.3.6. Transmission Electron Microscopy (TEM). Samples were prepared by putting a drop of BAIL solutions on the carbon-coated copper grid (300 mesh). Residual liquid was blotted immediately. Samples were imaged under a JEOL JEM-2100 electron microscope at a working voltage of 80 kV.

2.3.7. Synthesis and Characterization of Gold Nanostructures. Absorption spectra of gold sols were recorded on a UV−vis spectrophotometer (Cary 500, Varian). Scanning electron micrographs of the gold nanostructures were taken from a LEO 1430 VP Carl Zeiss scanning electron microscope. X-ray diffraction (XRD) patterns of the specimens were recorded by a Rigaku MiniFlex-II Desktop X-ray diffractometer (Ni-filtered Cu Kα radiation, k = 1.5404 Å).

3. RESULTS AND DISCUSSION

3.1. Tensiometry. Figure 1 shows the change in surface tension (γ) of water as a function of the concentration of various BAILs, 1,3-dialkylimidazolium alkyl sulfate ($[C_nH_{2n+1}mim][C_mH_{2m+1}OSO_3]$; n = 4, 6, or 8; m = 8, 12) at 298.15 K. In all the cases, γ decreases with the increase in BAIL concentration before reaching a constant value. The break points in the surface tension vs concentration plot give the critical aggregation concentration (CAC). Linear fits just before and after break points provided the CAC (Table 1). It has been observed that, with the increase in cationic chain length from n = 4 to 8, the CAC values decrease from 35 to 4 $mmol·kg^{-1}$ (~8-fold) when m = 8 and from 2.3 to 0.5 $mmol·kg^{-1}$ (~5-fold) when m = 12, indicating a significant improvement on the surface activity of BAILs with an increase in chain length of both the imidazolium counterion and anion. Because of the good electrical charge distribution, the sulfate group shows more propensity toward counterion binding.[50] The marked decrease in the CAC of BAILs is also due to high counterion binding of less hydrated imidazolium counterions (an increase of the chain length of imidazolium cation further reduces its hydration and enhances counterion binding) which offers effective screening between head groups.

The surface tension at CAC (γ_{CAC}) values obtained for BAILs are given in Table 1. The lower γ_{CAC} values indicate a densely packed arrangement of all BAILs at the air−water interface. The γ_{CAC} values obtained for lauryl sulfate (m = 12) based BAILs decreased in the following order: $[C_4mim]$ (34.4) > $[C_6mim]$ (27.1) > $[C_8mim]$ (26.0), and are lower than their sodium (34.9) or tetrapropylammonium (31.8) analogues.[51] These values are comparable to the amino acid based ionic liquid surfactants recently reported by our group.[21,39] A similar trend is followed by octyl sulfate (m = 8) based BAILs wherein the order is as follows: $[C_4mim]$ (26.1) > $[C_6mim]$ (25.6) > $[C_8mim]$ (24.4). The value of γ_{CAC} of BAILs is comparable to the lowest reported for imidazolium based trichain anionic surfactant $[C_4mim][TC]$[51] and analogous fluorocarbon surfactants.[51] The lowest γ_{CAC} value for $[C_8mim][C_8OSO_3]$ is due to good alkyl chain compatibility because of the same cationic and anionic alkyl chain length and is consistent with the previous observation that the lowest surface tensions are reached when the cation and anion tails are similar in size.[51] Low γ_{CAC} for BAILs as compared to the previously reported imidazolium based SAILs are indicative of a densely packed interface. As discussed earlier, the increased population of BAILs at the air−water interface is due to effective screening offered by the counterion, van der Waals interaction between alkyl chains of the cation and anion along with existing H-bonding and electrostatic interaction between sulfate and imidazolium

dx.doi.org/10.1021/jp309717n | J. Phys. Chem. B 2012, 116, 14363−14374

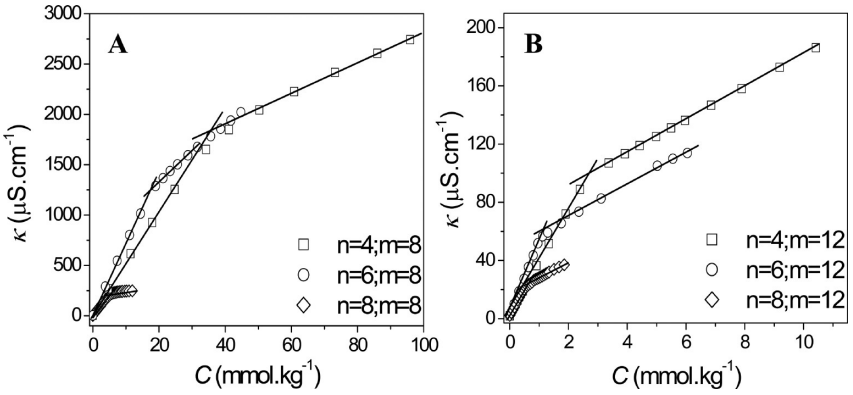

Figure 2. Plots of specific conductivity as a function of concentration of BAILs ($[C_nH_{2n+1}mim][C_mH_{2m+1}OSO_3]$) in aqueous solutions at 298.15 K.

Table 2. Critical Aggregation Concentration (CAC), Counterion Binding (β), Standard Gibbs Free Energy of Aggregation (ΔG°_{agg}), Enthalpy of Aggregation (ΔH°_{agg}), and Entropy of Aggregation (ΔS°_{agg}) of BAILs in an Aqueous Medium at Different Temperatures

$[C_nH_{2n+1}mim][C_mH_{2m+1}OSO_3]$							
n	m	T (K)	CAC (mmol·kg^{-1})	β	ΔG°_{agg} (kJ·mol^{-1})	ΔH°_{agg} (kJ·mol^{-1})	$T\Delta S^\circ_{agg}$ (kJ·mol^{-1})
4	8	288.15	38.5	0.70	−30.01	22.29	52.31
		298.15	35.8	0.71	−31.28	0.26	31.54
		308.15	35.0	0.71	−32.26	−20.35	11.91
		318.15	36.9	0.66	−32.14	−39.66	7.52
6	8	288.15	23.7	0.89	−35.11	5.55	40.66
		298.15	22.2	0.88	−36.49	0.59	37.08
		308.15	22.1	0.87	−37.56	−4.05	33.52
		318.15	23.1	0.88	−38.65	−8.39	30.25
8	8	288.15	5.8	0.91	−41.88	31.53	73.41
		298.15	5.6	0.94	−44.32	4.04	48.36
		308.15	5.7	0.91	−44.91	−21.66	23.25
		318.15	6.1	0.89	−45.71	−45.74	−0.04

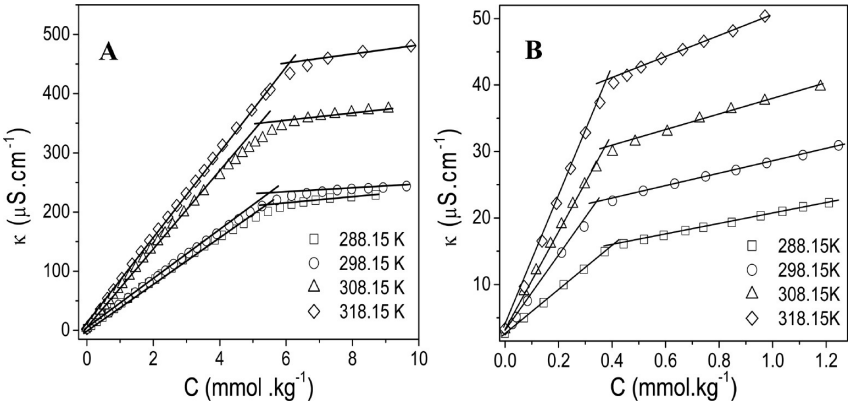

Figure 3. Temperature dependent conductivity profiles of aqueous-BAIL ($[C_nH_{2n+1}mim][C_mH_{2m+1}OSO_3]$) solutions: (A) n = 8; m = 8; (B) n = 8; m = 12.

moieties. The adsorption efficiency, pC_{20}, was calculated from surface tension vs concentration graphs using eq 1.

$$pC_{20} = -\log C_{20} \quad (1)$$

where C_{20} is the concentration required to reduce the surface tension of pure solvent by 20 mN·m^{-1}. A higher pC_{20} value is indicative of a higher adsorption efficiency of the surfactant at the interface and more efficiency in reducing surface tension. Surface pressure at CAC is defined as

$$\pi_{CAC} = \gamma_0 - \gamma_{CAC} \quad (2)$$

where γ_0 is the surface tension of pure solvent and γ_{CAC} is the surface tension of the solution at CAC. This parameter indicates the maximum reduction of surface tension caused by the dissolution of surfactant molecules and hence becomes a measure for the effectiveness of the surfactant to lower the surface tension of the solvent. The values of pC_{20} and π_{CAC} parameters obtained for the studied BAILs are given in Table 1. The adsorption efficiencies of BAILs with n = 4, 6, 8; m = 8 and n = 4; m = 12 are similar or even higher than conventional

dx.doi.org/10.1021/jp309717n | J. Phys. Chem. B 2012, 116, 14363−14374

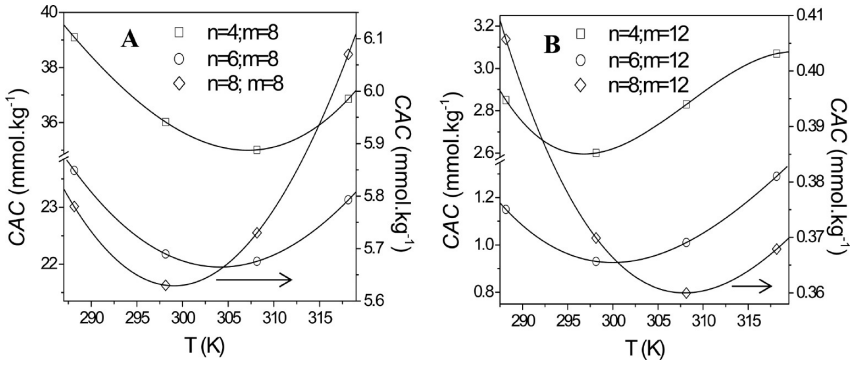

Figure 4. Temperature dependence of the CAC of BAILs ($[C_nH_{2n+1}mim][C_mH_{2m+1}OSO_3]$). ($n$ = 8 corresponds to the right y-axis, also marked by an arrow in parts A and B.)

Table 3. Critical Aggregation Concentration (CAC), Counterion Binding (β), Standard Gibbs Free Energy of Aggregation (ΔG°_{agg}), Enthalpy of Aggregation (ΔH°_{agg}), and Entropy of Aggregation (ΔS°_{agg}) of BAILs in an Aqueous Medium at Different Temperatures

$[C_nH_{2n+1}mim][C_mH_{2m+1}OSO_3]$							
n	m	T (K)	CAC (mmol·kg^{-1})	β	ΔG°_{agg} (kJ·mol^{-1})	ΔH°_{agg} (kJ·mol^{-1})	$T\Delta S^\circ_{agg}$ (kJ·mol^{-1})
4	12	288.15	2.9	0.69	−39.96	14.36	54.32
		298.15	2.6	0.69	−41.66	−2.65	39.01
		308.15	2.8	0.68	−42.53	−18.55	23.98
		318.15	3.1	0.67	−43.19	−33.46	9.73
6	12	288.15	1.1	0.80	−46.62	67.44	114.06
		298.15	0.9	0.82	−49.76	3.88	53.65
		308.15	1.0	0.79	−50.10	−55.54	−5.44
		318.15	1.3	0.75	−49.36	−111.24	−61.88
8	12	288.15	0.4	0.77	−50.11	93.09	143.21
		298.15	0.4	0.84	−54.31	45.31	99.62
		308.15	0.4	0.86	−56.80	0.61	57.42
		318.15	0.4	0.84	−58.06	−41.27	16.79

single chain surfactants or imidazolium based SAILs, whereas the BAILs with n = 6, 8; m = 12 show a somewhat higher adsorption efficiency which is comparable to amino acid ionic liquid surfactants.[8,15−21,52,53] Similarly, π_{CAC} of BAILs is comparable to the amino acid ionic liquid surfactants, whereas it is quite higher than conventional single chain surfactants or imidazolium based SAILs.[8,15−21,52,53]

The maximum surface excess concentration, Γ_{max}, and the area occupied by a single surfactant molecule at the air−water interface, A_{min}, of BAILs which are mainly dependent upon the size of the hydrophilic headgroup were estimated by applying the Gibbs adsorption isotherm to the surface tension data.[54,55] Fitting of γ values below the CAC to a second degree polynomial equation provided the slope required for estimation of Γ_{max}. The values of parameters derived from γ are reported in Table 1. Effective screening of like charge between head groups by the imidazolium counterions results in lowering of A_{min} which in turn causes an increase in Γ_{max}. The Γ_{max} values observed for BAILs are higher than SAILs[8,15−21] and conventional anionic surfactants having small as well as bulky organic counterions, like tetra alkyl ammonium ions.[56]

3.2. Conductometry. Conductivity measurements were performed at four different temperatures in the range 288.15−318.5 K. Plots of specific conductance, κ, as a function of BAIL ($[C_nH_{2n+1}mim][C_mH_{2m+1}OSO_3]$) concentration at 298.15 K are shown in Figure 2. The intersection of straight lines fitted for κ before and after slope change depicts the CAC. The CACs (Table 2) obtained for the BAILs from κ measurements are fairly in good agreement with the values obtained from γ values. Plots of the temperature dependence of κ vs concentration for the representative BAILs, $[C_8mim][C_8OSO_3]$ and $[C_8mim][C_{12}OSO_3]$, are shown in Figure 3A and B, respectively, whereas the plots for other BAILs are provided in the Supporting Information, Figure S1. Similar to the conventional surfactants[57] and imidazolium based SAILs,[58,59] a U-shape change in CAC was observed with an increase in temperature from 288.15 to 318.15 K for all studied BAILs (Figure 4). The ratio of the slope of linear fragments above and below the CAC gives an estimate of counterion binding, β. Estimated values of β for BAILs are given in Tables 2 and 3. Similar to the tetra alkyl ammonium salts, high values of β are observed for BAILs.[60] Expectedly, an increase in β has been observed with the increase in alkyl chain length of imidazolium cation because of enhanced hydrophobicity. Even higher values of β observed in the cases of $[C_8mim][C_8OSO_3]$ and $[C_8mim][C_{12}OSO_3]$ are due to the involvement of alkyl chains of both cation and anion in the aggregated structures. The standard Gibbs free energy of aggregation, ΔG°_{agg}, was calculated using the equation[61]

$$\Delta G^\circ_{agg} = (1 + \beta)RT \ln X_{CAC} \quad (3)$$

where X_{CAC} is the mole fraction of BAILs at the CAC. Negative ΔG°_{agg} indicates spontaneity of the process, Table 2. ΔG°_{agg} becomes more negative with the increase of the alkyl chain

dx.doi.org/10.1021/jp309717n | J. Phys. Chem. B 2012, 116, 14363−14374

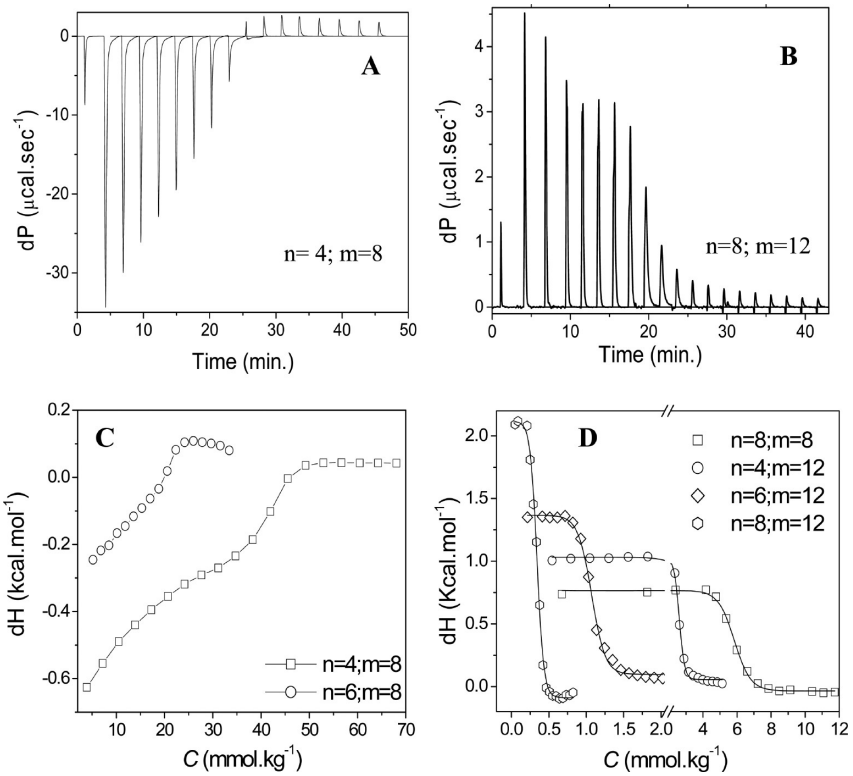

Figure 5. Calorimetric profiles of BAILs ($[C_nH_{2n+1}mim][C_mH_{2m+1}OSO_3]$) in aqueous solutions at 298.15 K. (A, B) Representative raw titration data of heat flow versus time, and (C, D) enthalpy of dilution as a function of the concentration of BAILs.

length of the cation and anion. When compared to conventional ILs/surfactants, the magnitude of ΔG°_{agg} for BAILs was found higher, indicating that the aggregation process is more feasible in these compounds.[19,22,24,33,57,60]

The enthalpy of aggregation, ΔG°_{agg}, was derived by applying the Gibbs–Helmholtz equation using the calculated free energy of aggregation

$$\Delta H^\circ_{agg} = \frac{\partial(\Delta G^\circ_{agg}/T)}{\partial(1/T)} \quad (4)$$

It has been observed that the changes in $\Delta G^\circ_{agg}/T$ with $1/T$ are nonlinear, and therefore, the slope was calculated through nonlinear second order curve fitting. Like conventional surfactants, the obtained ΔH°_{agg} was found to be positive at lower temperature and negative at higher temperature for all the studied BAILs (Tables 2 and 3).

Calculated values of ΔG°_{agg} and ΔH°_{agg} were used to estimate the standard entropy of aggregation from the following relation

$$\Delta S^\circ_{agg} = \frac{(\Delta H^\circ_{agg} - \Delta G^\circ_{agg})}{T} \quad (5)$$

Similar to ΔH°_{agg}, ΔS°_{agg} decreased with the increase in temperature for all the BAILs. For all the BAILs, a high magnitude of ΔS°_{agg} at low temperatures indicated that the aggregation process is mainly entropy driven, whereas it is enthalpy favored at high temperature.

3.3. Isothermal Titration Microcalorimetry (ITC). Isothermal calorimetric titration (ITC) was performed to measure the enthalpy changes upon aggregation, ΔH°_{agg}, for all BAILs ($[C_nH_{2n+1}mim][C_mH_{2m+1}OSO_3]$) at 298.15 K. Differential power (dP) values with time show exothermic and endothermic changes before and after CAC, respectively, for BAILs (n = 4, 6; m = 8), whereas only endothermic changes were observed for the BAILs (n = 8; m = 8, n = 4, 6, 8; m = 12) throughout the dilution process (the representative plots are given in Figure 5A,B, and plots of other BAILs are provided in the Supporting Information, Figure S2). BAILs with n = 4, 6; m = 8 followed type B enthalpograms, wherein a positive slope change in ΔH values was observed before the CAC and thereafter the ΔH acquired a plateau region, Figure 5C. Positive slope change in ΔH values for these BAILs is due to solute–solute interactions because of high CACs (35.2 and 17.9 mm, respectively). BAILs with n = 4, 6, or 8; m = 12 and n = 8; m = 8 exhibited two plateau regions in enthalpy values before and after the CAC (Figure 5D) which correspond to the type A enthalpograms.[62] Type A enthalpograms are known as textbook examples which exhibit constant ΔH changes before and after aggregation with a sharp change at the CAC. The CAC values obtained by the calorimetric method for all BAILs are reported in Table 4, and are in fairly good agreement with those obtained from conductivity and surface tension experiments. The observed ΔH°_{agg} was found to be positive for BAILs with n = 4; m = 8 and n = 6; m = 8, while it was negative for the other BAILs and the magnitude increased with the increase in substituted alkyl chain of imidazolium cation or alkyl sulfate anion following the order n = 8; m = 8 < n = 4; m = 12 < n = 6; m = 12 < n = 8; m = 12. Thermodynamic parameters (ΔG°_{agg}, ΔH°_{agg}, and ΔS°_{agg}) obtained from ITC are reported in Table 4. The thermodynamic parameters obtained from conductivity and calorimetric techniques differed in magnitude. The discrepancy arises due to contribution of a different physiochemical process other than the aggregation in calorimetric determination of enthalpy change.[63] The dynamic nature of the aggregation process and the counterion binding of aggregates are considered to influence the ΔH°_{agg} of the process

dx.doi.org/10.1021/jp309717n | J. Phys. Chem. B 2012, 116, 14363–14374

Table 4. Isothermal Titration Microcalorimetry Derived Critical Aggregation Concentration (CAC), Standard Gibbs Free Energy of Aggregation (ΔG°_{agg}), Enthalpy of Aggregation (ΔH°_{agg}), and Entropy of Aggregation (ΔS°_{agg}) of BAILs in an Aqueous Medium at 298.15 K

$[C_nH_{2n+1}mim][C_mH_{2m+1}OSO_3]$					
n	m	CAC ($mmol \cdot kg^{-1}$)	ΔG°_{agg} ($kJ \cdot mol^{-1}$)	ΔH°_{agg} ($kJ \cdot mol^{-1}$)	$T\Delta S^{\circ}_{agg}$ ($kJ \cdot mol^{-1}$)
4	8	34.7	−18.3	1.6	19.4
6	8	18.8	−20.1	0.7	20.8
8	8	5.4	−33.5	−3.3	30.2
4	12	2.6	−37.1	−4.3	32.8
6	12	1.1	−39.7	−5.1	34.6
8	12	0.4	−48.7	−9.8	38.9

which are usually not rigorously considered in conductivity data treatment. In the direct determination of the ΔH°_{agg} by calorimetry, the consequence of the above effects is, on the other hand, included in the measurement. ITC and κ measurements revealed that, similar to the conventional surfactants[63] and imidazolium based SAILs,[64] the aggregation process for the studied BAILs is entropy driven at 298.15 K.

3.4. Characterization of Self-Assembled Structures. Self-assembled structures of BAILs ($[C_nH_{2n+1}mim][C_mH_{2m+1}OSO_3]$) in aqueous medium were examined at a concentration 10 times to that of CAC. The hydrodynamic radii, R_h, of the aggregated structures measured from DLS are shown in Figure 6. DLS results show the formation of micelles in the aqueous solutions of $[C_4mim][C_8OSO_3]$ and $[C_6mim][C_8OSO_3]$, with R_h = 2.9 and 9.1 nm, respectively, whereas the aqueous solutions of $[C_4mim][C_{12}OSO_3]$ and $[C_6mim][C_{12}OSO_3]$ formed aggregates of micelles of R_h = 260.1 and 260.9 nm, respectively. TEM images (Figure 7A–D) also confirm formation of micelles and intermicellar structures. The higher hydrophobicity of lauryl sulfate along with a sufficiently longer alkyl chain of cation is perhaps the driving force for aggregation of micelles. The intermicellar aggregates are formed by bridging of imidazolium hydrophobic chains between individual micelles of lauryl sulfate similar to that reported for lauryl sulfate micelles by TBA+ ions, via hydrophobic interactions between butyl chains of the ions.[65] These intermicellar hydrophobic bridges could be easily broken with the addition of a simple electrolyte, such as NaCl. The effect of addition of NaCl on R_h of intermicellar aggregates of $[C_4mim][C_{12}OSO_3]$ and $[C_6mim][C_{12}OSO_3]$ is shown in the inset of Figure 6C. Aggregated micelles of $[C_4mim][C_{12}OSO_3]$ (R_h ~96 nm) and $[C_6mim][C_{12}OSO_3]$ (R_h ~113 nm) acquired individual micellar sizes of ~5 and 20 nm at 100 and 20 mM NaCl concentration, respectively (Figure 6C), indicating a higher propensity of the longer alkyl chain cation of the latter to participate in the aggregated structure. We speculate that the interactions of Cl^- ions with imidazolium cation in the palisade layer of micelles reduce the possibility of bridging of imidazolium hydrophobic alkyl tails resulting in separation of individual micelles. However, further investigations may be required to understand the exact mechanism of breaking of intermicellar aggregates under the influence of electrolytes.

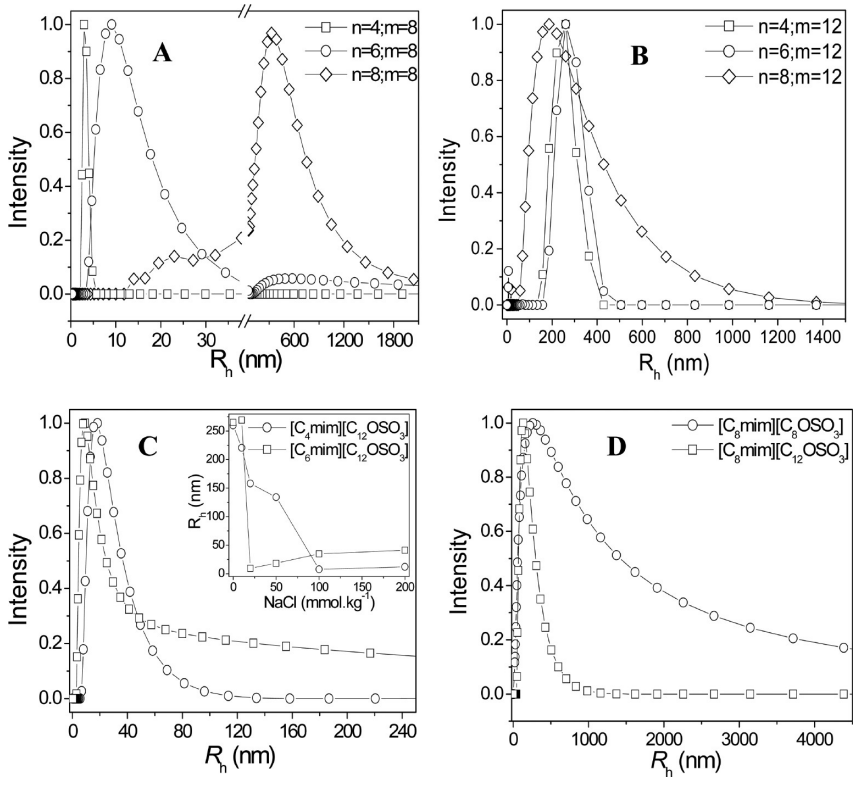

Figure 6. Size distribution of BAIL ($[C_nH_{2n+1}mim][C_mH_{2m+1}OSO_3]$) aggregates in water at a concentration 10 × CAC (A, B). Size distributions of $[C_4mim][C_{12}OSO_3]$ (□) and $[C_6mim][C_{12}OSO_3]$ (○) in 20 and 100 $mmol \cdot kg^{-1}$ aqueous NaCl solutions, respectively (the inset shows the variation in R_h at varying NaCl concentration) (C). Size distributions of $[C_8mim][C_8OSO_3]$ and $[C_8mim]$ $[C_{12}OSO_3]$ in 20 $mmol \cdot kg^{-1}$ aqueous NaCl solutions (D).

dx.doi.org/10.1021/jp309717n | J. Phys. Chem. B 2012, 116, 14363–14374

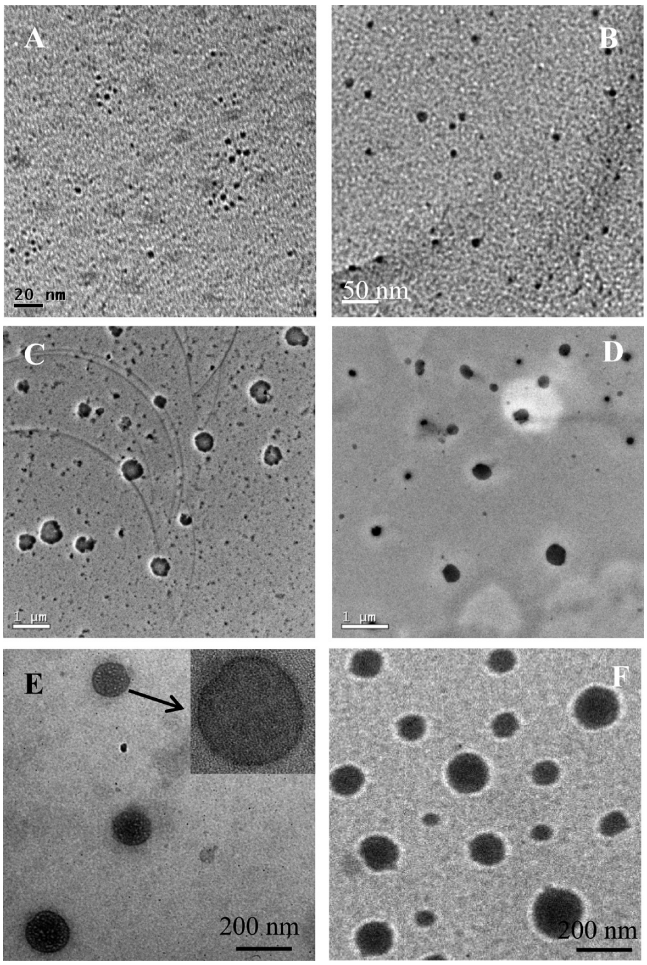

Figure 7. TEM images of micelles, aggregated micelles, and unilamellar vesicles formed by BAILs ($[C_nH_{2n+1}mim][C_mH_{2m+1}OSO_3]$) in water. (A, B) n = 4, 6; m = 8, (C, D) n = 4, 6; m = 12, and (E, F) n = 8; m = 8, 12.

The aqueous solutions of $[C_8mim][C_8OSO_3]$ or $[C_8mim][C_{12}OSO_3]$ were turbid and formed self-assembled structures with R_h = 328 and 187 nm, respectively, at the concentrations ~10 CAC (Figure 6), suggesting the formation of bilayer structures, such as vesicles. The vesicle size of $[C_8mim][C_8OSO_3]$ was found to grow as we increased the concentration above the CAC (Figure S3, Supporting Information). Alkyl chain compatibility in the case of C_8C_8 may be the reason for growth in vesicle size with the increase in concentration. Unlike intermicellar aggregates of $[C_4mim][C_{12}OSO_3]$ and $[C_6mim][C_{12}OSO_3]$, the structures formed in the aqueous solutions of $[C_8mim][C_8OSO_3]$ or $[C_8mim][C_{12}OSO_3]$ did not collapse with the addition of NaCl, suggesting the formation of vesicles in these BAILs, Figure 6D. Unilamellar vesicles formed by these BAILs were imaged from TEM (Figure 7E,F). The images recorded around the CAC showed nearly similarly sized spherical shaped vesicles for both $[C_8mim][C_8OSO_3]$ and $[C_8mim][C_{12}OSO_3]$. The self-assembled structures can be distinguished from NMR peak shapes of the cationic and anionic protons involved. Formation of compact and higher self-assembled structures, like vesicles,[66] leads to peak broadening because of restricted movement and shorter relaxation times of nuclei. Therefore, ^{1}H NMR spectra of aqueous BAIL solutions were recorded before and after the CAC. The changes in peak shapes of imidazolium ring protons are shown in Figure 8, and the changes for protons of the alkyl chain of both the cation and anion are shown in the Supporting Information (Figures S4 and S5). There is a clear peak broadening in aqueous solutions of $[C_8mim][C_8OSO_3]$ and $[C_8mim][C_{12}OSO_3]$ after the CAC, while in the other cases no change in peak shape is observed, indicating the vesicle formation in these BAILs (also evidenced from DLS and TEM). The broadening indicates the involvement of a cation along with an anion in the self-assembly. The balanced interactions between head groups, alkyl chains, and compatibility of alkyl chains of both of the ions (cation and anion) are responsible for the vesicle formation. The BAILs, $[C_4mim][C_{12}OSO_3]$ and $[C_6mim][C_{12}OSO_3]$, though they formed bigger structures, which are even bigger than the vesicles formed by $[C_8mim][C_{12}OSO_3]$, no broadening of NMR peaks, no turbidity in their aqueous solutions after the aggregation concentration, and reversal to individual micellar sizes after addition of an electrolyte unlike in the aqueous solutions of $[C_8mim][C_8OSO_3]$ or $[C_8mim][C_{12}OSO_3]$ rule out vesicle formation and confirm that these structures are intermicellar aggregates.

3.5. Synthesis of Gold Nanoparticles/Microplates in Aqueous BAIL Solutions. The aqueous solutions of BAIL micelles and vesicles were used as a medium for synthesis of gold nanostructures. 1 mM $HAuCl_4$ aqueous-BAIL solutions of varying BAIL concentrations ranging from just above the CAC to well above the CAC were prepared. Light (in micellar medium) and dark (in vesicular medium) yellow color aqueous solutions of $HAuCl_4$/BAILs were kept under UV lamp for photochemical reduction. Gold nanoparticle formation was monitored by visual observation of color change and confirmed by taking UV absorbance of reduced Au^{3+} ion solutions. The UV spectra of irradiated solutions of low and high BAIL concentrations are shown in Figure 9A and B, respectively. Absorbance peaks around 550 nm are indicative of the formation of gold nanostructures. It is observed that Au^{3+} ions were reduced to Au (0) in 10 min in the micellar medium, whereas a quite longer period of 4 h was required for the reduction process in the vesicular medium. SEM images (Figure 10A–D) revealed that nearly spherical nanoparticles of ~200 nm were formed at lower BAIL concentrations in all the solutions except that in the solutions containing $[C_8mim][C_8OSO_3]$, where some anisotropy was observed. With the increase of BAIL concentration in the solution, the propensity to form microplates increased and uniformly distributed microplates could be obtained at certain higher concentrations of all the BAILs except $[C_4mim][C_8OSO_3]$ and $[C_6mim][C_8OSO_3]$. Very thin microplates were formed in a micellar medium, whereas microplates of nearly 70 nm thickness were formed in vesicular solutions, Figure 10E–H. Gao et al. provided a probable mechanism of gold nanoparticle formation in imidazolium solutions wherein the imidazolium cation of BAILs interacts with gold precursor $AuCl_4^-$ ions through H-bond formation between ring protons and chlorine of $AuCl_4^-$ ions. The C=C olefinic bond of imidazolium formed in the process is readily oxidized into an epoxide, alcohol, and finally to a ketone by $AuCl_4^-$ into aqueous medium which are then adsorbed on the surface of Au particles and guiding to formation of nanostructured microsheets.[67] Figure 11 displays the X-ray diffraction (XRD) patterns of the representative samples prepared in a vesicular solution of low and high BAIL concentration. The peaks of the scattering angles (2θ) exhibit a

dx.doi.org/10.1021/jp309717n | J. Phys. Chem. B 2012, 116, 14363–14374

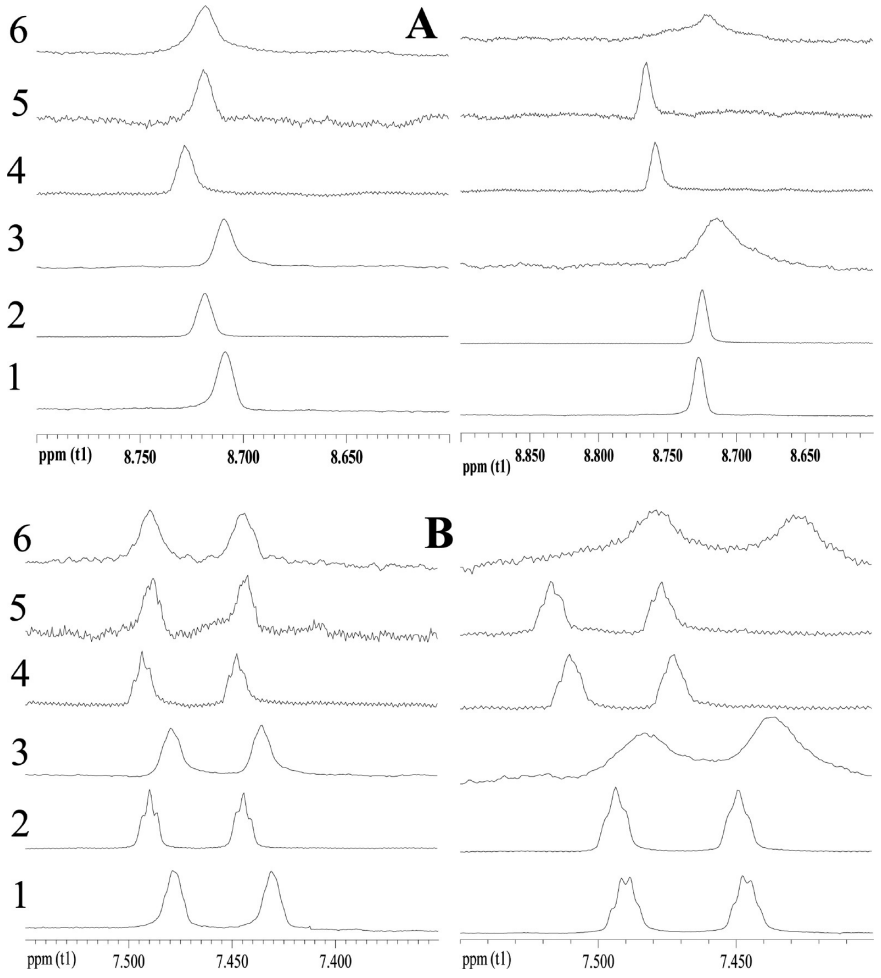

Figure 8. Changes in peak shapes of imidazolium ring protons, (A) 2H and (B) 4,5H of BAILs ($[C_nH_{2n+1}mim][C_mH_{2m+1}OSO_3]$) before (left) and after (right) aggregation. 1−3 (n = 4, 6, 8; m = 8) and 4−6 (n = 4, 6, 8; m = 12). Peak broadening in 3 and 6 is indicative of vesicle formation.

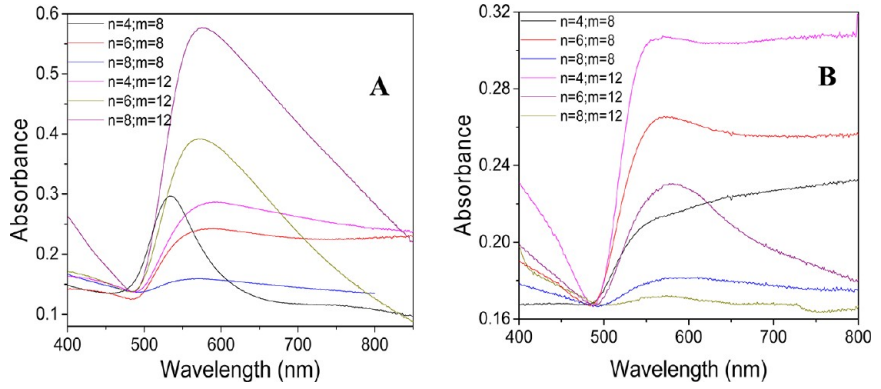

Figure 9. UV−vis/NIR spectrum of UV irradiated 1.0 mmol chloro auric acid solutions containing BAILs ($[C_nH_{2n+1}mim][C_mH_{2m+1}OSO_3]$). (A) ∼CAC and (B) ∼200 mmol·kg^{-1} (for n = 8; m = 12, the concentration was ∼70 mmol·kg^{-1}).

highly crystalline nature of gold nanostructures with a face-centered cubic (fcc) packing arrangement.

4. CONCLUSIONS

Biamphiphilic ionic liquids (BAILs) based on 1,3-dialkylimidazolium cation and alkyl sulfate anions ($[C_nH_{2n+1}mim][C_mH_{2m+1}OSO_3]$; n = 4, 6, or 8; m = 8, 12) have been synthesized and characterized for self-assembling behavior in their aqueous solutions. Synthesized BAILs have shown superior surface active properties than SAILs and conventional surfactants. The process of aggregation is found to be entropy driven at lower temperatures and enthalpy driven at higher temperatures for all the BAILs in the investigated temperature range. BAILs formed distinct aggregated structures depending on the amphiphilicity of the cation or anion. BAILs with butyl or hexyl substitution in imidazolium cation and having octyl sulfate as anion formed spherical micelles of R_h = 2.9 and 5.1 nm, whereas large intermicellar aggregates of R_h ∼260 nm were formed when the anion was replaced by lauryl sulfate. The

dx.doi.org/10.1021/jp309717n | J. Phys. Chem. B 2012, 116, 14363−14374

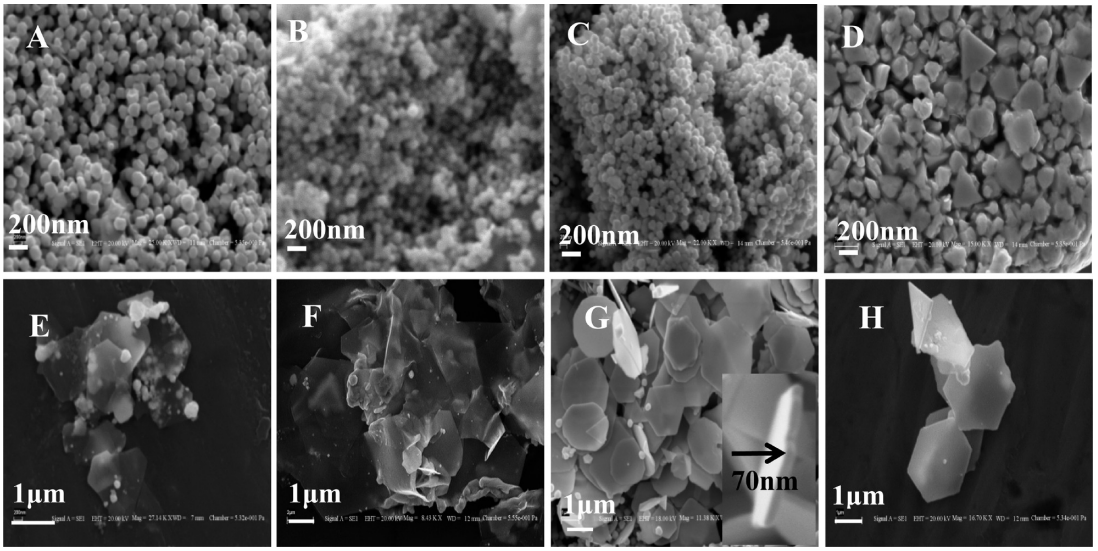

Figure 10. SEM images of gold nanoparticles and microplates synthesized by the photochemical method in aqueous BAILs ($[C_nH_{2n+1}mim][C_mH_{2m+1}OSO_3]$) solutions of lower (A–D) and higher concentrations (E–H), respectively. (A, E) $n = 4$; $m = 12$, (B, F) $n = 6$; $m = 12$, (C, G) $n = 8$; $m = 12$, and (D, H) $n = 8$; $m = 8$.

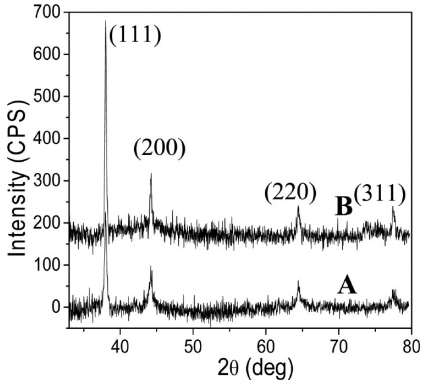

Figure 11. Representative X-ray diffraction pattern of gold nanostructures prepared in (A) low $[C_8mim][C_{12}OSO_3]$ concentration and (B) high $[C_8mim][C_{12}OSO_3]$ concentration solutions.

intermicellar aggregates could be reverted to individual micelles upon addition of an electrolyte. BAILs with octyl chain substituted imidazolium ions formed stable unilamellar vesicles. Micellar/vesicular solutions of BAILs have shown good potential for the synthesis of gold nanoparticles of controlled morphology. Nearly spherical nanoparticles were formed at low BAIL concentrations, whereas microplates could be obtained at high BAIL concentrations in the solutions under UV irradiation. Studies show that ILs can be tailored to achieve very high surface activity and to construct desired self-assembled structures for specific applications such as for the facile synthesis of nanomaterials of controlled morphology.

■ ASSOCIATED CONTENT

Supporting Information

Characterization of synthesized BAILs, temperature dependent conductivity (Figure S1), plots from ITC (Figure S2), DLS plot of R_h vs concentration (Figure S3), and NMR of alkyl chain protons (Figures S4 and S5). This material is available free of charge via the Internet at http://pubs.acs.org.

■ AUTHOR INFORMATION

Corresponding Author

*E-mail: mailme_arvind@yahoo.com; arvind@csmcri.org. Phone: +91-278-2567039. Fax: +91-278-2567562.

Notes

The authors declare no competing financial interest.

■ ACKNOWLEDGMENTS

K.S.R. is thankful to CSIR for a senior research fellowship. The authors are thankful to Department of Science and Technology (DST), Government of India, for financial support for this work (Nos. SR/S/PC-55/2008 and SR/S/PC-04/2010). The analytical division of CSMCRI is also acknowledged for helping in sample characterization. The authors thank Dr. Tejwant Singh for helpful discussions.

■ REFERENCES

(1) Wasserscheid, P., Welton, T., Eds. *Ionic Liquids in Synthesis*; Wiley-VCH: Weinheim, Germany, 2003.

(2) Chiappe, C.; Pieraccini, D. Ionic liquids: solvent properties and organic reactivity. *J. Phys. Org. Chem.* **2005**, *18*, 275–297.

(3) Huddleston, J. G.; Visser, A. E.; Matthew Reichert, W.; Willauer, H. D.; Broker, G. A.; Rogers, R. D. Characterization and comparison of hydrophilic and hydrophobic room temperature ionic liquids incorporating the imidazolium cation. *Green Chem.* **2001**, *3*, 156–164.

(4) Bowers, J.; Butts, P.; Martin, J.; Vergara-Gutierrez, C.; Heenan, K. Aggregation Behavior of Aqueous Solutions of Ionic Liquids. *Langmuir* **2004**, *20*, 2191–2198.

(5) Miskolczy, Z.; Sebok-Nagy, K.; Biczok, L.; Gokturk, S. Aggregation and micelle formation of ionic liquids in aqueous solution. *Chem. Phys. Lett.* **2004**, *400*, 296–300.

(6) Singh, T.; Kumar, A. Aggregation Behavior of Ionic Liquids in Aqueous Solutions: Effect of Alkyl Chain Length, Cations, and Anions. *J. Phys. Chem. B* **2007**, *111*, 7843–7851.

(7) Baltazar, Q. Q.; Chandawalla, J.; Sawyer, K.; Anderson, J. L. Interfacial and micellar properties of imidazolium-based monocationic and dicationic ionic liquids. *Colloids Surf., A* **2007**, *302*, 150–156.

(8) Dong, B.; Li, N.; Zheng, L.; Yu, L.; Inoue, T. Surface Adsorption and Micelle Formation of Surface Active Ionic Liquids in Aqueous Solution. *Langmuir* **2007**, *23*, 4178–4182.

(9) Zhao, Y.; Gao, S.; Wang, J.; Tang., J. Aggregation of Ionic Liquids [$C_n$mim] Br (n = 4, 6, 8, 10, 12) in D_2O: A NMR Study. *J. Phys. Chem. B* **2008**, *112*, 2031−2039.
(10) Blesic, M.; Lopes, A.; Melo, E.; Petrovski, Z.; Plechkova, N V.; Canongia Lopes, J. N.; Seddon, K. R.; Rebelo, L. P. N. On the Self-Aggregation and Fluorescence Quenching Aptitude of Surfactant Ionic Liquids. *J. Phys. Chem. B* **2008**, *112*, 8645−8650.
(11) Singh, T.; Kumar, A. Self-aggregation of ionic liquids in aqueous media: A thermodynamic study. *Colloids Surf., A* **2008**, *318*, 263−268.
(12) Wang, H.; Wang, J.; Zhang, S.; Xuan, X. Structural Effects of Anions and Cations on the Aggregation Behavior of Ionic Liquids in Aqueous Solutions. *J. Phys. Chem. B* **2008**, *112*, 16682−16689.
(13) Ao, M.; Xu, G.; Pang, J.; Zhao, T. Comparison of Aggregation Behaviors between Ionic Liquid-Type Imidazolium Gemini Surfactant [C_{12}-4-C_{12}im] Br_2 and Its Monomer [C_{12}mim] Br on Silicon Wafer. *Langmuir* **2009**, *25*, 9721−9727.
(14) Preiss, U.; Jungnickel, C.; Thoming, J.; Krossing, I.; Luczak, J.; Diedenhofen, M.; Klamt, A. Predicting the Critical Micelle Concentrations of Aqueous Solutions of Ionic Liquids and Other Ionic Surfactants. *Chem.—Eur. J.* **2009**, *15*, 8880−8885.
(15) Ao, M.; Xu, G.; Zhu, Y.; Bai, Y. Synthesis and properties of ionic liquid-type Gemini imidazolium surfactants. *J. Colloid Interface Sci.* **2008**, *326*, 490−495.
(16) Anouti, M.; Jones, J.; Boisset, A.; Jacquemin, J.; Caillon-Caravanier, M.; Lemordant, D. Aggregation behavior in water of new imidazolium and pyrrolidinium alkycarboxylates protic ionic liquids. *J. Colloid Interface Sci.* **2009**, *340*, 104−111.
(17) Ao, M.; Huang, P.; Xu, G.; Yang, X.; Wang, Y. Aggregation and thermodynamic properties of ionic liquid-type gemini imidazolium surfactants with different spacer length. *Colloid Polym. Sci.* **2009**, *287*, 395−402.
(18) Li, X.; Gao, Y.; Liu, J.; Zheng, L.; Chen, B.; Wub, L.; Tung, C. Aggregation behavior of a chiral long-chain ionic liquid in aqueous solution. *J. Colloid Interface Sci.* **2010**, *34*, 94−101.
(19) Shi, L.; Li, N.; Yan, H.; Gao, Y.; Zheng, L. Aggregation Behavior of Long-Chain N-Aryl Imidazolium Bromide in Aqueous Solution. *Langmuir* **2011**, *27*, 1618−1625.
(20) Dong, B.; Gao, Y.; Su, Y.; Zheng, L.; Xu, J.; Inoue, T. Self-Aggregation Behavior of Fluorescent Carbazole-Tailed Imidazolium Ionic Liquids in Aqueous Solutions. *J. Phys. Chem. B* **2010**, *114*, 340−348.
(21) Rao, K. S.; Singh, T.; Trivedi, T. J.; Kumar, A. Aggregation Behavior of Amino Acid Ionic Liquid Surfactants in Aqueous Media. *J. Phys. Chem. B* **2011**, *115*, 13847−13853.
(22) Brown, P.; Butts, C. P.; Eastoe, J.; Fermin, D.; Grillo, I.; Lee, H.; Parker, D.; Plana, D.; Richardson, R. M. Anionic Surfactant Ionic Liquids with 1-Butyl-3-methyl-imidazolium Cations: Characterization and Application. *Langmuir* **2012**, *28*, 2502−2509.
(23) Liu, X.; Dong, L.; Fang, Y. Synthesis and Self-Aggregation of a Hydroxyl-Functionalized Imidazolium-Based Ionic Liquid Surfactant in Aqueous Solution. *J. Surfactants Deterg.* **2011**, *14*, 203−210.
(24) Zhao, M.; Zheng, L. Micelle formation by N-alkyl-N-methylpyrrolidinium bromide in aqueous solution. *Phys. Chem. Chem. Phys.* **2011**, *13*, 1332−1337.
(25) Singh, T.; Rao, K. S.; Kumar, A. Effect of Ethylene Glycol and its Derivatives on Aggregation Behaviour of an Ionic Liquid 1-Butyl-3-Methyl Imidazolium Octylsulfate in Aqueous Medium. *J. Phys. Chem. B* **2012**, *116*, 1612−1622.
(26) Bhadani, A.; Singh, S. Synthesis and Properties of Thioether Spacer Containing Gemini Imidazolium Surfactants. *Langmuir* **2011**, *27*, 14033−14044.
(27) Thomaier, S.; Kunz, W. Aggregates in mixtures of ionic liquids. *J. Mol. Liq.* **2007**, *130*, 104−107.
(28) Li, N.; Zhang, S. H.; Zheng, L. Q.; Dong, B.; Li, X. W.; Yu, L. Aggregation behavior of long-chain ionic liquids in an ionic liquid. *Phys. Chem. Chem. Phys.* **2008**, *10*, 4375−4377.
(29) Kang, W.; Dong, B.; Gao, Y.; Zheng, L. Aggregation behavior of long-chain imidazolium ionic liquids in ethylammonium nitrate. *Colloid Polym. Sci.* **2010**, *288*, 1225−1232.
(30) Huang, R. T. W.; Peng, K. C.; Shih, H. N.; Lin, G. H.; Chang, T. F.; Hsu, S. J.; Hsu, T. S. T.; Lin, I. J. B. Antimicrobial properties of ethoxyether-functionalized imidazolium salts. *Soft Matter* **2011**, *7*, 8392−8400.
(31) Chamiot, B.; Rizzi, C.; Gaillon, L.; Sirieix-Plenet, J.; Lelievre, J. Redox-Switched Amphiphilic Ionic Liquid Behavior in Aqueous Solution. *Langmuir* **2009**, *25*, 1311−1315.
(32) Jiao, J.; Dong, B.; Zhang, H.; Zhao, Y.; Wang, X.; Wang, R.; Yu, L. Aggregation Behaviors of Dodecyl Sulfate-Based Anionic Surface Active Ionic Liquids in Water. *J. Phys. Chem. B* **2012**, *116*, 958−965.
(33) Cornellas, A.; Perez, L.; Comelles, F.; Ribosa, I.; Manresa, A.; Garcia, M. T. Self-aggregation and antimicrobial activity of imidazolium and pyridinium based ionic liquids in aqueous solution. *J. Colloid Interface Sci.* **2011**, *355*, 164−171.
(34) Rao, V. G.; Ghosh, S.; Ghatak, C.; Mandal, S.; Brahmachari, U.; Sarkar, N. Designing a new strategy for the formation of IL-in-oil microemulsion. *J. Phys. Chem. B* **2012**, *116*, 2850−2855.
(35) Zech, O.; Thomaier, S.; Bauduin, P.; Ruck, T.; Touraud, D.; Kunz, W. Microemulsions with an Ionic Liquid Surfactant and Room Temperature Ionic Liquids As Polar Pseudo-Phase. *J. Phys. Chem. B* **2009**, *113*, 465−473.
(36) Freire, M. G.; Neves, C. M. S. S.; Canongia Lopes, J. N.; Marrucho, I. M.; Coutinho, J. A. P.; Rebelo, L. P. N. Impact of Self-Aggregation on the Formation of Ionic-Liquid-Based Aqueous Biphasic Systems. *J. Phys. Chem. B* **2012**, *116*, 7660−7668.
(37) Pino, V.; German-Hernandez, M.; Martin-Perez, A.; Anderson, J. L. Ionic Liquid-Based Surfactants in Separation Science. *Sep. Sci. Technol.* **2012**, *47*, 264−276.
(38) Galan, M. C.; Tran, A. T.; Boisson, J.; Benito, D.; Butts, C.; Eastoe, J.; Brown, P. [R_4N][AOT]: A Surfactant Ionic Liquid as a Mild Glycosylation Promoter. *J. Carbohydr. Chem.* **2011**, *30*, 486−497.
(39) Trivedi, T. J.; Rao, K. S.; Singh, T.; Mandal, S. K.; Sutradhar, N.; Panda, A. B.; Kumar, A. Task-Specific, Biodegradable Amino Acid Ionic Liquid Surfactants. *ChemSusChem* **2011**, *4*, 604−608.
(40) Kim, K.; Choi, S.; Cha, J.; Yeon, S.; Lee, H. Facile one-pot synthesis of gold nano particles using alcohol ionic liquids. *J. Mater. Chem.* **2006**, *16*, 1315−1317.
(41) Bai, X.; Gao, Y.; Liu, H.; Zheng, L. Synthesis of Amphiphilic Ionic Liquids Terminated Gold Nanorods and Their Superior Catalytic Activity for the Reduction of Nitro Compounds. *J. Phys. Chem. C* **2009**, *113*, 17730−17736.
(42) Souza, B. S.; Leopoldino, E. C.; Tondo, D. W.; Dupont, J.; Nome, F. Imidazolium-Based Zwitterionic Surfactant: A New Amphiphilic Pd Nanoparticle Stabilizing Agent. *Langmuir* **2012**, *28*, 833−840.
(43) Singh, K.; Marangoni, D. G.; Quinn, J. G.; Singer, R. D. Spontaneous vesicle formation with an ionic liquid amphiphile. *J. Colloid Interface Sci.* **2009**, *335*, 105−111.
(44) Yuan, J.; Bai, X.; Zhao, M.; Zheng, L. C_{12}mimBr Ionic Liquid/SDS Vesicle Formation and Use As Template for the Synthesis of Hollow Silica Spheres. *Langmuir* **2010**, *26*, 11726−11731.
(45) Rao, K. S.; Singh, T.; Kumar, A. Aqueous-Mixed Ionic Liquid System: Phase Transitions and Synthesis of Gold Nanocrystals. *Langmuir* **2011**, *27*, 9261−9269.
(46) Singh, T.; Drechsler, M.; Müller, A. H. E.; Mukhopadhyay, I.; Kumar, A. Micellar transitions in the aqueous solutions of a surfactant-like ionic liquid: 1-butyl-3-methylimidazolium octyl sulfate. *Phys. Chem. Chem. Phys.* **2010**, *12*, 11728−11735.
(47) Obliosca, J. M.; Arco, S. D.; Huang, M. H. Synthesis and Optical Properties of 1-Alkyl-3-Methylimidazolium Lauryl Sulfate Ionic Liquids. *J. Fluoresc.* **2007**, *17*, 613−618.
(48) Santos, C. S.; Baldelli, S. Alkyl Chain Interaction at the Surface of Room Temperature Ionic Liquids: Systematic Variation of Alkyl Chain Length (R) C1-C4, C8) in both Cation and Anion of [RMIM][R-OSO_3] by Sum Frequency Generation and Surface Tension. *J. Phys. Chem. B* **2009**, *113*, 923−933.
(49) Blesic, M.; Swadzba-Kwasny, M.; Holbrey, J. D.; Canongia Lopes, J. N.; Seddon, K. R.; Rebelo, L. P. N. New catanionic surfactants based on 1- alkyl-3-methyl imidazolium alkylsulfonates,

[C_nH_{2n+1}mim][$C_mH_{2m+1}SO_3$]: mesomorphism and aggregation. *Phys. Chem. Phys. Chem.* **2009**, *11*, 4260−4268.
(50) Zana, R.; Schmidt, J.; Talmon, Y. Tetrabutylammonium Alkyl Carboxylate Surfactants in Aqueous Solution: Self-Association Behavior, Solution Nanostructure, and Comparison with Tetrabutylammonium Alkyl Sulfate Surfactants. *Langmuir* **2005**, *21*, 11628−11636.
(51) Brown, P.; Butts, C.; Dyer, R.; Eastoe, J.; Grillo, I.; Guittard, F.; Rogers, S.; Heenan, R. Anionic Surfactants and Surfactant Ionic Liquids with Quaternary Ammonium Counterions. *Langmuir* **2011**, *27*, 4563−4571.
(52) Pitt, A. R.; Morley, S. D.; Burbidge, N. J.; Quickenden, E. L. The relationship between surfactant structure and limiting values of surface tension, in aqueous gelatin solution, with particular regard to multilayer coating. *Colloids Surf., A* **1996**, *114*, 321−325.
(53) Dong, B.; Zhao, X.; Zheng, L.; Zhang, J.; Li, N.; Inoue, T. Aggregation behavior of long-chain imidazolium ionic liquids in aqueous solution: Micellization and characterization of micelle microenvironment. *Colloids Surf., A* **2008**, *317*, 666−672.
(54) Rosen, M. J. *Surfactants and Interfacial Phenomena*, 2nd ed.; Wiley:New York, 1989.
(55) Jaycock, M. J.; Parfitt, G. D. *Chemistry of Interfaces*; John Wiley and Sons: New York, 1981.
(56) Tadmouri, R.; Zedde, C.; Routaboul, C.; Micheau, J. C.; Pimienta, V. Partition and Water/Oil Adsorption of Some Surfactants. *J. Phys. Chem. B* **2008**, *112*, 12318−12325.
(57) Benrraou, M.; Bales, B. L.; Zana, R. Effect of the Nature of the Counterion on the Properties of Anionic Surfactants. 1. Cmc, Ionization Degree at the Cmc and Aggregation Number of Micelles of Sodium, Cesium, Tetramethylammonium, Tetraethylammonium, Tetrapropylammonium, and Tetrabutylammonium Dodecyl Sulfates. *J. Phys. Chem. B* **2003**, *107*, 13432−13440.
(58) Kang, K. H.; Kim, H. U.; Lim, K. H. Effect of temperature on critical micelle concentration andthermodynamic potentials of micellization of anionicammonium dodecyl sulfate and cationic octadecyl trimethyl ammonium chloride. *Colloids Surf., A* **2001**, *189*, 113−121.
(59) Inoue, T.; Ebina, H.; Dong, B.; Zheng, L. Electrical conductivity study on micelle formation of long-chain imidazolium ionic liquids in aqueous solution. *J. Colloid Interface Sci.* **2007**, *314*, 236−241.
(60) Luczak, J.; Jungnickel, C.; Joskowska, M.; Thoming, J.; Hupka, J. Thermodynamics of micellization of imidazolium ionic liquids in aqueous solutions. *J. Colloid Interface Sci.* **2009**, *336*, 111−116.
(61) Rosen, M. J. *Surfactant and Interfacial Phenomenon*, 2nd ed.; John Wiley and Sons: New York, 1988.
(62) Bijma, K.; Engberts, J. B. F. N.; Blandamer, M. J.; Cullis, P. M.; Last, P. M.; Irlam, K. D.; Giorgio Soldi, L. Classfication of calorimetric titration plots for alkyltrimethylammonium and alkylpyridinium cationic surfactants in aqueous solutions. *J. Chem. Soc., Faraday Trans.* **1997**, *93*, 1579−1584.
(63) Chatterjee, A.; Moulik, S. P.; Sanyal, S. K.; Mishra, B. K.; Puri, P. M. Thermodynamics of Micelle Formation of Ionic Surfactants: A Critical Assessment for Sodium Dodecyl Sulfate, Cetyl Pyridinium Chloride and Dioctyl Sulfosuccinate (Na Salt) by Microcalorimetric, Conductometric, and Tensiometric Measurements. *J. Phys. Chem. B* **2001**, *105*, 12823−12831.
(64) Geng, F.; Liu, J.; Zheng, L.; Yu, L.; Li, Z.; Li, G.; Tung, C. Micelle Formation of Long-Chain Imidazolium Ionic Liquids in Aqueous Solution Measured by Isothermal Titration Microcalorimetry. *J. Chem. Eng. Data* **2010**, *55*, 147−151.
(65) Zana, R.; Benrraou, M.; Bales, B. L. Effect of the Nature of the Counterion on the Properties of Anionic Surfactants. 3. Self-Association Behavior of Tetrabutylammonium Dodecyl Sulfate and Tetradecyl Sulfate: Clouding and Micellar Growth. *J. Phys. Chem. B* **2004**, *108*, 18195−18203.
(66) Villeneuve, M.; Ootsu, R.; Ishiwata, M.; Nakahara, H. Research on the Vesicle-Micelle Transition by ^{1}H NMR Relaxation Measurement. *J. Phys. Chem. B* **2006**, *110*, 17830−17839.
(67) Gao, Y.; Voigt, A.; Zhou, M.; Sundmacher, K. Synthesis of Single-Crystal Gold Nano- and Microprisms Using a Solvent-Reductant-Template Ionic Liquid. *Eur. J. Inorg. Chem.* **2008**, *24*, 3769−3775.